Neutron diffuse scattering study of the ferromagnetism in Pt–10 at. % Fe

P. Radhakrishna, H. M. Gilder, G. Parette, and A. Menelle
Laboratoire Léon Brillouin, Laboratoire Commun du Commissariat à l'Energie Atomique et du Centre National de la Recherche Scientifique, Centre d'Etudes Nucléaires de Saclay, 91191 Gif-sur-Yvette CEDEX, France
(Received 12 December 1988; revised manuscript received 9 February 1989)

We have measured the neutron diffuse scattering between 20 and 217 K from an alloy of Pt–10 at. % Fe for scattering vectors $Q=4\pi\sin\theta/\lambda$ in the range 0.2 Å^{-1} > Q > 0.058 Å^{-1} at a neutron wavelength of $\lambda=4.76$ Å. The scattering at 20 K was accounted for by the presence of two types of microdomains of 25 and 57 Å radii, respectively. The magnetic moment of the larger cluster was estimated to be $\approx 100\mu_B$. The critical exponent ν, the Curie temperature T_C, and the characteristic inverse correlation length κ_0 were derived from a least-squares fit of the data to the Fischer-Burford-based expression for the scattering cross section. After correction for inelastic effects, the best estimates of the critical parameters were found to be $\nu=0.75\pm0.03$, $T_C=159.5\pm0.5$ K, and $\kappa_0=0.324\pm0.015$ Å^{-1}. This alloy would therefore appear to belong to the universal class of magnetic materials known as the three-dimensional Heisenberg model ($\nu=0.70$). Mean-field theory ($\nu=\frac{1}{2}$) obviously does not hold for this system.

I. INTRODUCTION

Alloys of platinum and palladium containing small concentrations of 3*d* solutes such as Fe, Ni, Co, or Mn are isotropic metallic ferromagnets which are of interest for both theoretical[1–4] and experimental[2,5] reasons. Special attention has been focused on the onset and distribution[5] of magnetization at low temperatures, and on the longitudinal and transverse susceptibilities at higher temperatures[6] near the Curie point in these systems.

We thus present the results of an investigation of diffuse neutron scattering from a typical alloy of this class, namely Pt–10 at. % Fe. In previous studies, the ferromagnetism at low temperatures was interpreted[7] in terms of giant magnetic clusters consisting of localized moments on the magnetic solute atoms, surrounded by induced moments on atoms of the host. However, much less is known about the coalescence of these giant moments into large ferromagnetic microdomains which account for the neutron scattering observed in similar dilute alloys.[5] Our objective was to characterize these entities in Pt–10 at. % Fe, as well as to measure the parameters describing the critical scattering near the Curie temperature in this isotropic metallic system.

As Cowley has indicated,[8] the critical exponents associated with certain classes of materials are dependent only on the symmetry, dimensionality, and range of the interactions. The influence of such universal criteria overrides other obvious differences (metal versus insulator, antiferromagnet versus ferromagnet, etc.). This is more than adequately illustrated by $RbMnF_3$, EuO, and EuS, which all belong to the same universal class. In Sec. IV B, we will show that an analysis of the data available on the alloys PdFe and PdMn appears to indicate that they also belong to this class.

In the context of these considerations, it therefore seemed of interest to investigate a dilute alloy of PtFe, provided that the concentration of iron could be chosen in such a way as to allow sufficient separation between critical scattering and that due to magnetic clusters. Both contributions are obviously associated with certain characteristic temperatures. The characteristic temperature T_{Cl} associated with the formation of giant clusters is related to $J_{\mathrm{RKKY}}(R_b)$, the Ruderman-Kittel-Kasuya-Yosida interaction evaluated at the spin bond length,[5] or equivalently at the average solute-solute separation R_b. Inasmuch as $J_{\mathrm{PtFe}}\cong 93\pm24$ K at first-nearest-neighbor separations,[3] $J_{\mathrm{RKKY}}(R_b)<93$ K, provided that $R_b > a/\sqrt{2}$, a being the lattice parameter. On the other hand, the Curie temperature T_C of dilute PtFe alloys depends on the atomic concentration of iron c through the relation[9,10] $T_C\cong 1.6\times10^3(C-0.0076)$. Adequate separation between T_{Cl} and T_C would thus be expected, *a priori*, in Pt–10 at. % Fe, since $T_C\approx150$ K and $R_b\approx 2a$.

II. EXPERIMENTAL PROCEDURE

The sample consisted of a single crystal of Pt–10 at. % Fe, 12 mm in diameter and about 10 cm long, and made from 99.990% pure materials. A single crystal was not necessary for our purposes, but was conveniently available. It was positioned vertically along the "2θ" axis of the diffuse scattering spectrometer *G*6–1 at the research reactor "Orphée" operated by the Léon Brillouin Laboratory, Saclay, France. A wavelength of $\lambda=4.76$ Å, selected by a graphite monochromator, was used for the measurements. The sample was attached to the cold finger of a closed-cycle cryorefrigerator. A multicounter assembly of 400 units, referred to as a "banana," detected the scattered neutrons. Each unit covered an angle of 0.2°. The direct beam prevented the collection of useable data in the first five or six detectors, i.e., it was not possible to get closer than about 1° to the forward-scattering direction. Nevertheless, the minimum value of the wave vector Q

was 0.058 $Å^{-1}$, typical of the usual utilization of the spectrometer $G6-1$. Data was collected up to a maximum value of $Q \approx 0.2$ $Å^{-1}$. Since no energy discrimination was used, it was thus necessary to use an elaborate correction procedure in order to ascertain the quasielastic scattering component (see Sec. IV B). The temperature and run times were automatically controlled.

The data were transmitted to and stored in a microcomputer, thus permitting subsequent processing and analysis. Corrections for the background, fast neutrons, counter efficiency, etc., were applied by using the results of similar runs in which the sample was either totally absent or replaced by a cadmium absorber. A standard vanadium scatterer was used to normalize the data, thus allowing the cross sections to be expressed in absolute units of b/sr.

III. EXPERIMENTAL RESULTS

A. Low-temperature data

A typical scattering curve of intensity $I(Q)$ versus Q at low temperatures is shown in Fig. 1. The data corresponds to a temperature of 20 K. The slight hump in the curve at $Q = 0.085$ $Å^{-1}$ occurring after the upswing at the lowest values of Q, is present at all of the temperatures for which data were acquired. The solid line is a fit to the data and will be discussed below (see Sec. IV A).

In Fig. 2 we show the variation of the magnetic susceptibility, or equivalently, $I(Q)/T$, with T, Q being fixed at each of the three smallest values measured. We note a steep upturn in $I(Q)/T$ at low temperatures ($T < 80$ K). This effect, in a region of decreasing "critical" susceptibility, presumably reflects the presence of extended regions of correlated spins.[2]

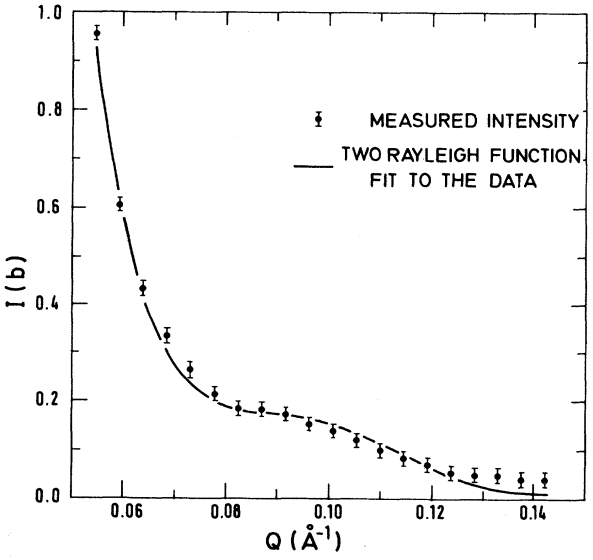

FIG. 1. Scattered-neutron intensity as a function of scattering vector Q at $T = 20$ K in the ferromagnetic phase.

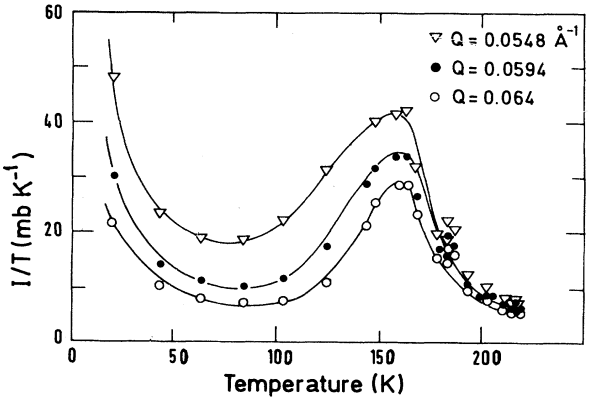

FIG. 2. Scattered-neutron intensity divided by temperature as a function of temperature for the three lowest values of the scattering vector Q.

B. High-temperature data

Those neutron scattering runs for which the forward-scattered intensity decreased with increasing temperature were used to describe the critical scattering near and above T_C in the paramagnetic region of the alloy. There were 11 such runs ranging from 167.7 to 217.3 K. The position of the "banana" allowed intensity measurements at scattering vectors Q ranging from 0.05 to 0.17 $Å^{-1}$.

Given the experimental precision of 0.015 b in the measurements, no statistically significant variation of the scattering cross section with temperature could be observed in the four highest-temperature runs for which $T > 210$ K. Thus, the data shown in Fig. 3 represent the average of four runs effected between 210 and 217 K.

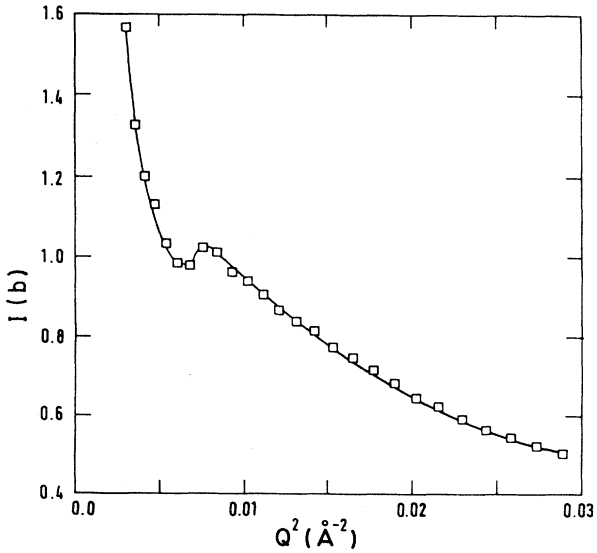

FIG. 3. Scattered-neutron intensity in the paramagnetic phase as a function of scattering vector squared Q^2 at $T > 210$ K averaged over the four highest-temperature runs. The error bars are the size of the symbols (□).

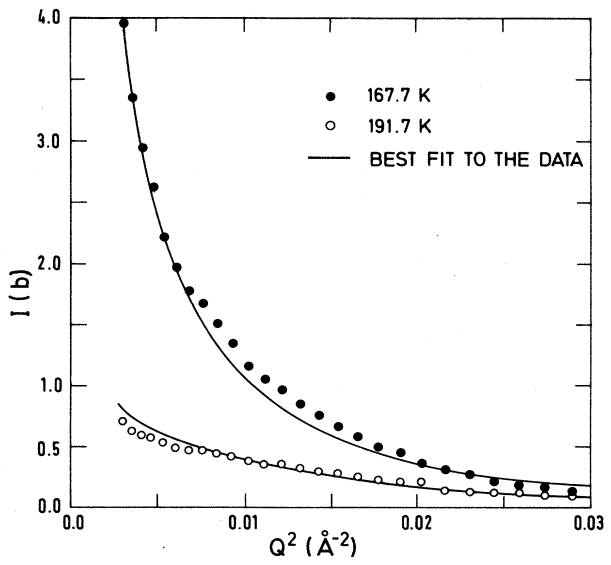

FIG. 4. Scattered-neutron intensity as a function of Q^2 at $T=167.7$ and 191.7 K. The intensities represent the difference between the measured values and those of Fig. 3, and thus correspond to the critical scattering only. The solid lines are best fits based on $\nu=0.75$, $T_C=159.6$ K, and $\kappa_0=0.324$ Å^{-1}. The error bars are the size of the symbols representing the data (□ and ○).

The pronounced hump in the data appearing at $Q\approx 0.08$ Å^{-1} is magnetic in origin (see Sec. IV A). These highest-temperature data are then subtracted from the other runs, the "difference" data being indicative of critical scattering.

Only the four lowest-temperature runs closest to the ferromagnetic transition, namely 16.7, 177.4, 182.1, and 191.7 K, provided differences large enough to reliably ascertain the critical parameters of interest. Figure 4 shows the difference data for $T=167.7$ and 191.7 K. The solid curves represent fits to the data (see discussion in Sec. IV B). We notice the absence of the hump in the difference data. The data shown in Fig. 4 are corrected for inelastic effects (see discussion in Sec. IV B).

IV. DISCUSSION

A. Low-temperature results

The experimental evidence for giant ferromagnetic moments of induced magnetization on the platinum atoms surrounding the localized moments of the iron atom has been reviewed by Ododo[7] and Muellner.[11] However, a fit of the present data to a single Rayleigh-function form factor representing scattering from a population of identical spherical clusters or microdomains of radius R was inadequate to explain our results due to the additional scattering represented by the hump at $Q=0.085$ Å^{-1}. The near equality of the coherent scattering lengths of platinum and iron ($b_{\rm Pt}=9.5$ fm, $b_{\rm Fe}=9.54$ fm) eliminates the direct contribution due to nuclear scattering. Since the number of scattering centers associated with the hump changes above the Curie temperature (see Sec. IV B), the hump is clearly magnetic in origin. Thus, the observed scattering can be described by two groups of magnetic entities embedded in a paramagnetic matrix. The first group presumably consists of randomly oriented ferromagnetic microdomains. It seems plausible that the second group consists of "spin-reversed" regions, as has been previously suggested.[2] These regions in which some of the spins tend to cancel are likely since antiferromagnetic interactions occur in Pt_3Fe. However, no further direct characterization of the properties of these magnetic entities is possible based on the present data. The groups are distinguished by different magnetic moments, hence different characteristic temperatures, as evidenced by the observed persistence of the hump above the Curie temperature.

Assuming, as a first approximation, that scattering due to interparticle correlations is negligible, the small-angle scattering cross section is given by the sum of two terms:[12]

$$\frac{d\sigma}{d\Omega}(Q)=\sum_i \omega_i F_i^2(QR_i)\ ,$$

where (1)

$$w_i=\tfrac{2}{3}(\gamma e^2/2mc^2)^2 C_i(1-C_i)\mu_i^2\ .$$

Now γ is just the gyromagnetic ratio of the neutron, e^2/mc^2 is the classical radius of the electron, and C_i, μ_i, F_i, and R_i are the concentration, magnetic moment, Rayleigh-function form factor, and radius of the ith species, respectively ($i=1,2$). The factor of $\frac{2}{3}$ arises from the assumed random orientation of the scatterers. In addition, $F_i(0)=1$.

A least-squares fit of the data to Eq. (1) yields the following values of the parameters of interest: $R_1=25.4$ Å, $R_2=57.2$ Å, $w_1=0.464$ b/sr, and $w_2=6.58$ b/sr. The entire function representing the measured neutron scattering is then given by

$$\frac{d\sigma}{d\Omega}=4.18\left[\frac{\sin(25.4Q)-(25.4Q)\cos(25.4Q)}{(25.4Q)^3}\right]^2 +59.2\left[\frac{\sin(57.2Q)-(57.2Q)\cos(57.2Q)}{(57.2Q)^3}\right]^2 . \quad (2)$$

Figure 1 shows the more than satisfactory agreement between this expression and the experimental data. Although this model seems oversimplified in its neglect of a continuous distribution of cluster sizes and scattering due to interference between clusters, we will see later that it is probably justified (see Sec. IV B).

The best-fit values correspond to magnetic clusters of 25 and 57 Å, respectively. This identification is based on the observation that the larger domains persist above the Curie temperature (see Sec. IV B).

Inasmuch as the present scattering data only allow a determination of the product of C_i and μ_i^2, we can nevertheless estimate an upper limit for C_i and thus a lower limit for μ_i. At some threshold value of C_i interference effects must inevitably modify the form of Eq. (2).

Guinier[13] has shown that the form factor $F_i^2(QR_i)$ for independent-particle scattering in the infinitely dilute limit should be multiplied by a factor of the form $[1+8C_iF_i(2QR_i)]^{-1}$. As $F_i \to 0$ as $Q \to \infty$, interference effects will obviously be most noticeable for $QR_i \ll 1$. In fact, when this factor is incorporated in Eq. (2), and C_i is made to vary between 0 and 0.52 (maximum packing fraction on a simple-cubic lattice), the scattering intensity only changes significantly below $Q \approx 0.08$ Å^{-1}. By imposing the condition that the calculated intensity should not differ by more than two standard deviations from the measured values, we were able to set an upper limit on the concentration of the larger of the two domains. Inasmuch as the variation of the intensity due to a change of concentration of the smaller domains was five times less than that of the larger ones, an upper limit for their concentration could not be determined. Specifically, for the larger domains, $(C_2)_{\max} \approx 10^{-2}$, and from Eq. (1),

$$(\mu_2)_{\min} = [\tfrac{3}{2}(2\ mc^2/\gamma e^2)^2/C_2]^{0.5} \approx 10^2 \mu_B \ .$$

Corresponding quantities cannot be ascertained for the smaller domains. The concentration is in order of magnitude agreement with that found in CuNi[12] ($2-7\times10^{-3}$) and RhNi[7] (6×10^{-3}), whereas the magnetic moment associated with these randomly oriented microdomains is considerably larger than those generally previously reported. It is of interest to note that Acker and Huguenin[14] have also reported large magnetic moments lying between 40 and 220μ_B in $Ni_{40}Cu_{60}$. It is possible that our data can be fitted on the basis of more than one model, most of them more elaborate (including, for instance, a distribution of cluster sizes, etc.) than the one presently employed.

B. High-temperature data

The theoretical expression describing the critical neutron scattering results from combining the Fischer-Burford[15] formulation of the Q-dependent static susceptibility with the usual formalism[16,17] for magnetic neutron scattering. This leads to the following expression:

$$\frac{d\sigma}{d\Omega}(Q,T) = \left[\frac{AT}{\kappa_1^2+Q^2}\right]^{1-\eta/2} , \tag{3a}$$

where

$$\kappa_1 = \kappa_0(T/T_c - 1)^{\nu} , \tag{3b}$$

and where A is a constant independent of temperature T and scattering vector Q, T_C is the Curie temperature, η and ν are critical exponents, and κ_1 is the inverse correlation length. "κ_0" is just a characteristic inverse correlation length. Equation (3) obviously reduces to the mean-field description[18] of critical scattering for $\eta=0$ and $\nu=0.5$. As $\eta \ll 1$ is often found to be the case in many other materials,[19] we assume that $\eta=0$ in the present analysis. Thus, by fitting the scattering data to Eq. (3), least-squares values of T_C, ν, and κ_0 can be determined. Any statistically significant departure from $\nu=0.5$ would then imply an alloy behavior incompatible with mean-field theory.

Inasmuch as only the ten smallest scattering vectors at each of the four temperatures were considered, 40 experimental points in all were used to perform the fit to Eq. (3).

However, Eq. (3) describes only the quasielastic scattering of neutrons by the thermal fluctuations of the magnetization, not taking account of the inelastic-scattering events. Previous studies[20,21] of critical neutron scattering in iron have shown that the measured cross section can be in error by as much as 10–20 % if not appropriately corrected[22,23] for the inelastic contribution. The correction factor depends on the scattering angle θ, the inverse correlation length κ_1, and the spin-diffusion constant Λ, and can be easily calculated by numerical methods *once these parameters are specified.* Inasmuch as κ_1 is to be determined in the present experiment, and Λ has never been measured for the alloy under consideration, it was necessary to use an iterative calculation procedure starting with the best-fit value of κ_1 (i.e., κ_0, T_C, and ν) determined from fitting Eq. (3) to the uncorrected data ($\Lambda=0$). Least-squares values of the parameters in Eq. (3) were then calculated as a function of Λ, the correct value of the parameters corresponding to that value of Λ that minimizes χ^2. Being guided by the experimentally determined value of $\mu \cong 11$ ($\mu \equiv 2m\Lambda/h$, m and h being the neutron mass and Planck's constant, respectively) for iron,[20,23] μ, the dimensionless spin-diffusion coefficient, was thus varied between 0 and 15 in the present analysis.

Figure 5 shows that the best least-squares fit occurs at a value of $\mu \cong 7$. The inelastic correction clearly improves the fit between the data and the elastic cross section of Eq. (3), as can clearly be seen by comparing χ^2 at

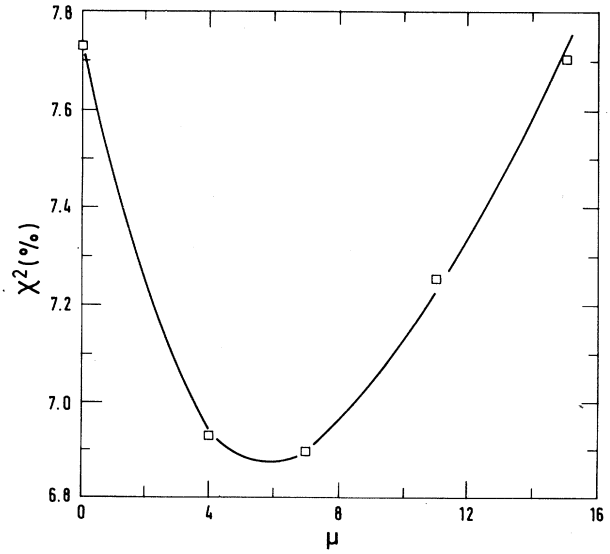

FIG. 5. χ^2 as a function of the dimensionless spin-diffusion coefficient μ.

$\mu=0$ (the purely elastic-scattering limit) to that at $\mu=7$.

The parameters of interest, namely T_C, ν, and κ_0, are shown as a function of μ in Fig. 6. Given the intrinsic standard deviations of the parameters corresponding to a particular value of μ, i.e., $\delta\nu\cong 0.03$, $\delta T_C\cong 0.5$ K, and $\delta\kappa_0\cong 0.015$ Å^{-1}, a linear variation of ν, T_C, and κ_0 with μ was assumed. The best estimates of the "critical" parameters are thus $T_c=159.5\pm 0.5$ K, $\nu=0.75\pm 0.03$, and $\kappa_0=0.324\pm 0.015$ Å^{-1}.

The fits to the data at 167.7 and 191.7 K, as shown in Fig. 4, are based on these values. Even the data beyond the first ten points are extremely well fit by the calculated curves, as inspection of Fig. 4 reveals. The quality of the fit decreases with increasing temperature and hence decreasing signal, as would be expected. The fit is indeed satisfactory, inasmuch as the fractional standard deviation is 0.068, totally consistent with the experimental uncertainty in the measured cross sections. On the other hand, when the data are not corrected for the presence of the larger clusters, the fractional standard deviation is 0.11, that is, almost twice as big.

In Fig. 7 we have calculated the total scattering cross section at 214 K due to the larger magnetic clusters [second term of Eq. (2)] and the critical scattering given by Eq. (3) as a function of Q^2. Excellent agreement between Figs. 7 and 3 is obtained by doubling the number of the larger magnetic clusters while using the low-temperature value of the radius. Specifically, we are able to account for the hook at $T>T_C$. It arises from the first maximum in the Rayleigh function whose prominence indicates a relatively narrow distribution of the radius characterizing the larger of the two types of clusters. This lends additional weight to our method of treating the high-temperature data.

The presently measured value of $T_C=159.5\pm 0.5$ K can be compared to previous measurements based on low-field susceptibility[9,10] on alloys containing comparable iron concentration. A chemical analysis of the sample used in the present experiment yielded a concentration of 9.47 ± 0.08 at % Fe, uniformly distributed to within the indicated precision. At this impurity concentration, the available data[9,10] indicate that the Curie temperature most probably lies between 143 and 164 K. Our value is obviously in good agreement with these results.

The characteristic inverse correlation length κ_0 is the limiting value of the temperature-dependent inverse correlation length κ_1 at temperatures well above the Curie temperature. In particular, according to Eq. (3b), $\kappa_1=\kappa_0$ at $T=2T_C$. At this temperature the spins are expected to be correlated up to a distance $1/\kappa_0$ not exceeding the nearest-neighbor separation of $a/\sqrt{2}$. This would predict $\kappa_0\approx\sqrt{2}/a=\sqrt{2}/3.9=0.36$ Å^{-1}, in gratifying agreement with the value of $\kappa_0=0.324$ Å^{-1} presently experimentally determined.

The critical exponent ν obviously differs significantly from the mean-field value of $\frac{1}{2}$. Cowley has pointed out[8] that the concept of the universality of phase transitions implies that the temperature dependence of the properties of a system close to T_C is the same for all materials of the same class, while differing from one universal class of

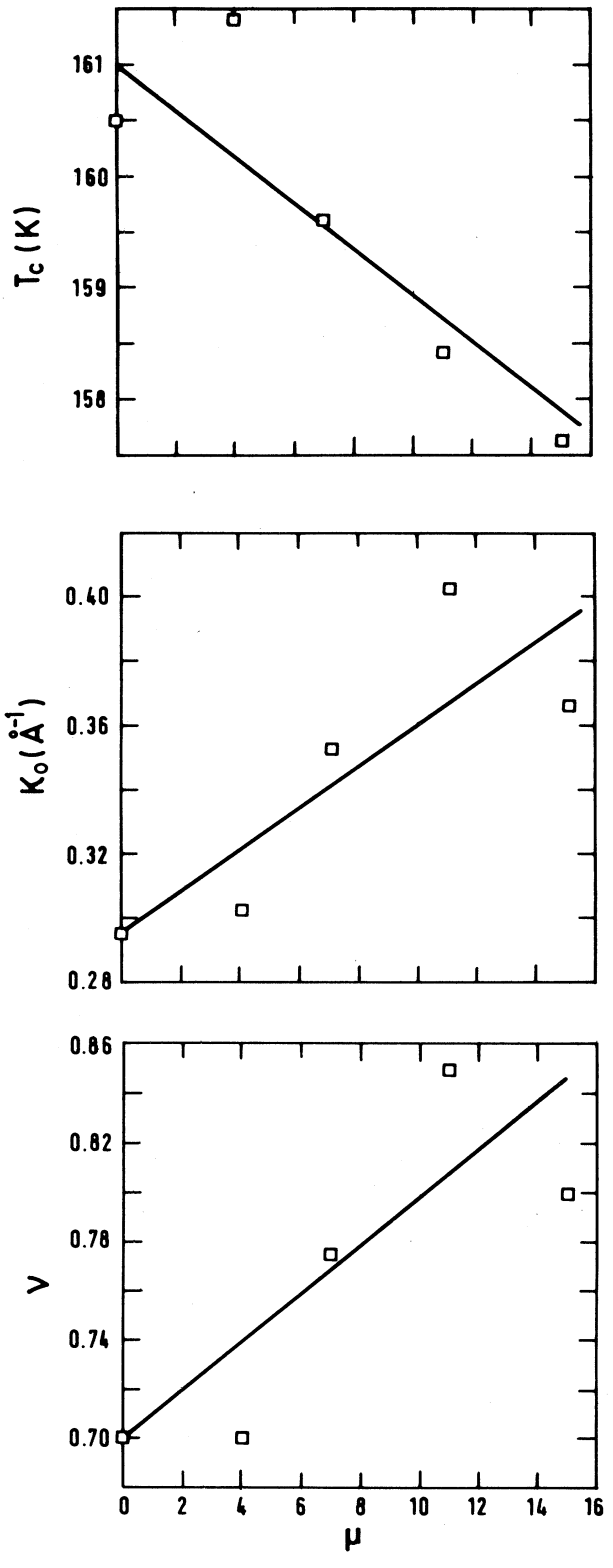

FIG. 6. The Curie temperature T_C, the critical exponent ν, and the characteristic inverse correlation length κ_0 as a function of the spin-diffusion coefficient μ. The straight lines are a guide to the eye.

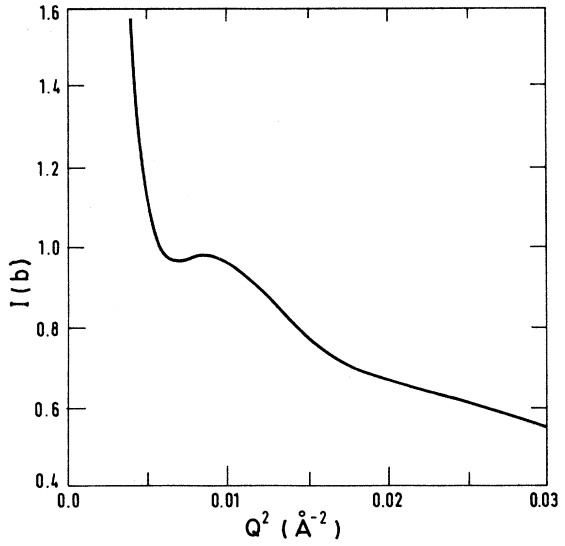

FIG. 7. Calculated scattered-neutron intensity in the paramagnetic phase as a function of scattering vector squared Q^2 at $T > 210$ K. The intensity is the sum of the contributions of the Rayleigh function describing the scattering from the larger microdomains and that due to the residual critical scattering.

materials to another. Based on the value of $\nu = 0.75 \pm 0.03$, alone, it would appear that the presently studied dilute alloy, Pt–10 at. % Fe, would belong to the universal class of isotropic, three-dimensional Heisenberg magnets, for which theory[24] predicts $\nu = 0.702$. Other members of this class, as pointed out by Cowley,[8] are the insulating antiferromagnet $RbMnF_3$ (Ref. 25) ($\nu = 0.701 \pm 0.011$), and the insulating ferromagnets EuO (Ref. 26) ($\nu = 0.681 \pm 0.017$) and EuS (Ref. 26) ($\nu = 0.702 \pm 0.022$).

In fact, the dilute, metallic ferromagnets Pd–2 at. % Mn, Pd–0.5 at % Fe, and Pd–0.25 at. % Fe would also appear to take their place alongside Pd–10 at. % Fe in this class, inasmuch as a fit of previously published data[5] for these alloy systems to Eq. (3b) results in the following values of the critical exponent ν: 0.7 ± 0.2, 0.77 ± 0.07, and 0.6 ± 0.1 for Pd–2 at. % Mn, Pd–0.5 at. % Fe, and Pd–0.25 at. % Fe, respectively. For pure iron itself the measured values of ν are 0.64 ± 0.02 (Ref. 21) and 0.77 ± 0.08.[27] Evidently, a number of magnetically inhomogeneous, dilute ferromagnetic metallic alloys, the pure element iron, and insulating antiferromagnetic and ferromagnetic salts have roughly the same critical exponent ν. In this context, the present result, which shows a deviation from mean-field theory, would appear to be entirely reasonable.

V. CONCLUSIONS

In conclusion, we have used diffuse neutron scattering to elucidate certain features of the inhomogeneous nature of the ferromagnetic state, as well as details of critical scattering phenomena in the dilute alloy of Pt–10 at. % Fe. This was made possible by an appropriate choice of the scattering characteristics and solute concentration of the alloy. We have shown that at low temperatures, the scattering can be interpreted in terms of two types of microdomains, of 25 and 57 Å radii, respectively, the latter carrying magnetic moment of the order of $100\mu_B$.

The present work represents one of the few attempts to extract critical exponents from neutron scattering in an isotropic metallic ferromagnet. It has been shown that this alloy belongs to the universal class of three-dimensional Heisenberg magnets,[8] since $\nu = 0.75 \pm 0.03$. This result underlines the importance of symmetry and dimensionality in critical phenomena. In this context, recent experimental work[28,29] on topological considerations of symmetry have indicated that frustrated systems imply the existence of new universal classes. We feel that continued work on critical exponents in systems possessing unusual spin configurations will provide additional information on phase transitions in the future.

ACKNOWLEDGMENTS

The authors are grateful to Dr. R. Bellissent for his critical reading on the manuscript and to Dr. M. Hennion for her useful comments. Special thanks are given to M. Pilier of the Commisariat à l'Energie Atomique (CEA Fontenay-aux-Roses) for her rapid analyses of the sample used in the experiments. We also take this opportunity to thank the CEA, and the Centre National de la Recherche Scientifique (CNRS) for their joint support of this work.

[1] J. C. Ododo, J. Phys. F **10**, 2515 (1980).
[2] J. C. Ododo, J. Phys. F **12**, 1821 (1982).
[3] A. C. Gonzalez and R. Parra, J. Appl. Phys. **55**, 2045 (1984).
[4] R. Medina, R. E. Parra, G. Mora, and A. C. Gonzalez, Phys. Rev. B **32**, 1628 (1985).
[5] B. H. Verbeek *et al.*, Phys. Rev. B **22**, 5426 (1980).
[6] P. W. Mitchell, R. A. Cowley, and R. Pynn, J. Phys. F **17**, L875 (1984).
[7] J. C. Ododo, Solid State Commun. **25**, 493 (1978).
[8] R. A. Cowley, *Methods of Experimental Physics; Neutron Scattering* (Academic, New York, 1987), Vol. 2, Part C, p. 1.
[9] J. C. Ododo, J. Phys. F **9**, 1441 (1979).
[10] R. Segnan, Phys. Rev. **160**, 404 (1967).
[11] W. C. Muellner and J. C. Kouvel, Phys. Rev. B **11**, 4552 (1975).
[12] T. J. Hicks, B. Rainford, J. S. Kouvel, and G. G. Low, Phys. Rev. Lett. **22**, 11 (1969); **22**, 531 (1969).
[13] A. Guinier and G. Fournet, *Small-Angle Scattering of X-Rays* (Wiley, New York, 1955), p. 48.
[14] F. Acker and R. Huguenin, Phys. Lett. **38A**, 5 (1972); **38A**, 343 (1972).
[15] M. E. Fisher and R. J. Burford, Phys. Rev. **156**, 583 (1967).
[16] W. Marshall and S. W. Lovesey, *Theory of Thermal Neutron Scattering* (Clarendon, Oxford, 1971), p. 467.
[17] G. Parette, Ann. Phys. (Paris) **T7**, 4 (1972); **T7**, 299 (1972).
[18] L. S. Ornstein and F. Zernike, Z. Phys. **27**, 761 (1926).

[19]G. Parette, Ann. Phys. (Paris) **T7**, 5 (1972); **T7**, 313 (1972).
[20]B. Jacrot, J. Konstantinovic, G. Parette, and D. Cribier, *Inelastic Scattering of Neutrons in Solids and Liquids* (Vienna, IAEA, 1963), Vol. 2, p. 317.
[21]L. Passell, K. Blinowski, T. Brun, and P. Nielsen, Phys. Rev. **139**, 1866 (1965).
[22]D. Bally, B. Grabcev, A. M. Lungu, M. Popovici, and M. Totia, J. Phys. Chem. Solids **28**, 1947 (1967).
[23]P. Nielsen, Danish Atomic Energy Commission Research Establishment Risö Report No. 118, 1965.
[24]E. J. Squires, Proc. Phys. Soc. London **67**, 248 (1954).
[25]A. Tucciarone, H. Y. Lau, L. M. Corliss, A. Delapalme, and J. M. Hastings, Phys. Rev. B **4**, 3206 (1971).
[26]O. W. Dietrich, J. Als-Nielsen, and L. Passell, Phys. Rev. B **14**, 4923 (1976).
[27]G. Parette and R Kahn, J. Phys. (Paris) **32**, 447 (1971).
[28]H. Kadowaki, S. M. Shapiro, T. Inami, and Y. Ajiro, J. Phys. Soc. Jpn. **57**, 2640 (1988).
[29]Y. Ajiro, T. Nakashima, Y. Unno, H. Kadowaki, M. Mekata, and N. Achiwa, J. Phys. Soc. Jpn. **57**, 2648 (1988).